



**pH- and redox-responsive self-assembly of amphiphilic
hyperbranched poly(amido amine)s for controlled
doxorubicin delivery**

Journal:	<i>Biomaterials Science</i>
Manuscript ID:	BM-ART-11-2014-000410.R1
Article Type:	Paper
Date Submitted by the Author:	08-Jan-2015
Complete List of Authors:	Cheng, Weiren; Institute of Materials Research and Engineering, Kumar, Jatin; Institute of Materials Research and Engineering, Zhang, Yong; National University of Singapore, Division of Bioengineering Liu, Ye; Institute of Materials Research and Engineering,

ARTICLE

pH- and redox-responsive self-assembly of amphiphilic hyperbranched poly(amido amine)s for controlled doxorubicin delivery

Cite this: DOI: 10.1039/x0xx00000x

Weiren Cheng,^{a,b} Jatin N. Kumar,^a Yong Zhang,^b and Ye Liu^{a*}Received 00th January 2012,
Accepted 00th January 2012

DOI: 10.1039/x0xx00000x

www.rsc.org/

Vinyl-terminated hyperbranched poly(amido amine)s is obtained from Michael addition polymerization of 4-(aminomethyl)piperidine (AMPD) with a double molar *N,N*-cystaminebis(acrylamide) (BAC). Then amphiphilic hyperbranched poly(BAC2-AMPD1)-PEG is produced via converting the vinyl groups to amines followed by PEGylation. Transmission electron microscopy (TEM), dynamic light scattering (DLS), and ¹H nuclear magnetic resonance (NMR) results indicate that the micelles can be obtained via self-assembly of hyperbranched poly(BAC2-AMPD1)-PEG. Further anti-cancer drug, doxorubicin (DOX), can be loaded into the micelles. pH- and redox-response of the micelles of hyperbranched poly(BAC2-AMPD1)-PEG without and with DOX are investigated. The results of confocal microscopy and flow cytometry reflect that FITC tagged or DOX loaded micelles of hyperbranched poly(BAC2-AMPD1)-PEG can enter HepG2 and MCF-7 cells, and DOX can be observed in the nucleus of the cells. The cytotoxicity of the micelles without and with DOX is evaluated in HepG2 and MCF-7 cells, and the efficacy to kill the cancer cells is discussed in comparison with free DOX.

Introduction

pH- and/or redox-responsive polymer drug delivery systems are promising for cancer treatment due to the lower pH environment of tumor and the significantly higher reduction potential in intracellular compartments.^{1,2} The concentration of the representative reducing compound, glutathione (GSH), is 100-1000 times higher in the intracellular apartments than in extracellular matrixes.^{3,4} Typically, pH- responsive polymers contain amino⁵⁻⁷ or imidazole groups,⁸⁻¹⁰ acetal linkage¹¹ or hydrazine linkage¹²⁻¹⁶ which can be protonated or hydrolyzed under acidic condition respectively; and majority of the redox-responsive polymers contain disulfide bonds.^{7,17,18} Drug delivery systems can be formulated either by conjugating drugs to polymers covalently¹⁹⁻²² or loading the drugs into assemblies of polymers which are widely obtained via self-assembly of amphiphilic linear or branched polymers.^{7,23-25} So far, majority of polymer drug delivery systems are from linear polymers, and few are from hyperbranched polymers. Due to the unique structures of hyperbranched polymers, it is attractive to develop more types of hyperbranched polymer drug delivery systems.

Poly(amido amine)s show low hemolytic activity and peptide-mimicking properties and have been explored for preparation of drug, gene and imaging agent delivery systems.^{7,26-32} pH- and redox- responsive poly(amido amine)s can be prepared via Michael addition polymerization of disulfide containing acrylic monomer with amines.^{31,34} Our previous works indicates the reactivity sequence of the three

types of amines of trifunctional amines in Michael Addition polymerization with acrylic monomers,^{7,35-37} and both linear and hyperbranched poly(amino ester)s and poly(amido amine)s are obtained via Michael addition polymerization of trifunctional amines with acrylic monomers.^{7,17,35-40} Amphiphilic linear poly(amino amine)s was developed and explored for pH- and redox-responsive delivery of doxorubicin (DOX)⁷ and imaging agents,⁴⁰ and hyperbranched poly(amido amine)s was explored for gene delivery,¹⁷ and preparation of well controlled hydrogel.³¹

Here we report a novel pH- and redox- responsive drug delivery systems obtained from self-assembly of amphiphilic hyperbranched poly(amido amine)s which is prepared by the approach shown in Scheme 1. Vinyl-terminated hyperbranched poly(BAC2-AMPD1) is synthesized via Michael addition polymerization of 4-(aminomethyl)piperidine (AMPD) with a double molar *N,N*-cystaminebis(acrylamide) (BAC). Then the vinyl terminal group is converted to primary amine via the reaction with excess AMPD, and poly(ethylene glycol) (PEG) is conjugated to some of the terminal amino groups to form amphiphilic hyperbranched poly(BAC2-AMPD1)-PEG. pH- and redox-responsive micelles can be obtained via self-assembly of hyperbranched poly(BAC2-AMPD1)-PEG in aqueous solution, and are applied for encapsulation and delivery of anti-cancer drug, DOX. pH- and redox-responsive properties of the micelles without or with DOX are evaluated,

and the efficacy of DOX loaded micelles to kill cancer cells are demonstrated.

Scheme 1

Experimental Section

Materials

N,N-cystaminebis(acrylamide) (BAC) from Polysciences, 4-(aminomethyl)piperidine (AMPD) from Alfa Aesar, doxorubicin hydrochloride (DOX-HCl) from Fluka Analytical, and L-glutathione reduced (GSH), fluorescein isothiocyanate (FITC) and buthionine sulphoximine (BSO) from Sigma Aldrich were used as received. Monomethyl poly(ethylene glycol) (PEG) (~2000 g/mol) 4-nitrophenyl carbonate was prepared following our previous report.⁴¹ Methanol, ethanol, dimethylsulfoxide (DMSO), and other solvents were purchased from Tedia and used as received. MCF-7 (human breast adenocarcinoma) cells and HepG2 (human hepatoma) cells from American Type Culture Collection (ATCC, Rockville, MD) were maintained in Dulbecco's modified eagle medium (DMEM, invitrogen) with 10% fetal bovine serum (FBS), 2 mM glutamine, 100 units/ml penicillin and 100 µg/ml streptomycin at 37 °C in an incubator with 5% CO₂ atmosphere.

Synthesis of hyperbranched poly(BAC2-AMPD1)

In a typical procedure, 2.36 g (20.4mmol) of AMPD in 10 mL of ethanol was added dropwise to 10.58g (40.6mmol) of BAC in 50 ml of ethanol at 65 °C under argon. After 14 days, the reaction solution was added dropwise into 11.79 g (101.9 mmol) of AMPD in 60 mL of anhydrous DMSO at room temperature under argon. 24 h later, the solution was dialyzed using dialysis membrane with a molecular weight cut-off of 3500 in methanol. To monitor the polymerization, a small amount of the reaction solution was dried and then dissolved in methanol-d₄ for ¹³C nuclear magnetic resonance (NMR) experiments with the total monomer concentrations being kept at ca. 25% (w/v). ¹³C NMR spectra were obtained using a power-gated decoupling program (PD) with 200 times scan taking ca.10 minutes.

Synthesis of amphiphilic hyperbranched poly(BAC2-AMPD1)-PEG

In a typical experiment, 3.93 g (1.7mmol) of monomethyl PEG(~2000 g/mol) 4-nitrophenyl carbonate was added to 6.86 g (18.3mmol) of hyperbranched poly(BAC2-AMPD1) in 55 mL of anhydrous DMSO. The solution was stirred for 5 days at room temperature under argon followed by dialysis using membrane with a molecular weight cut-off of 10 000 in methanol.

Formation and characterization of micelles of hyperbranched poly(BAC2-AMPD1)-PEG

9 mL of deionized water was added at a rate of 0.5 mL/h using a syringe pump to 20 mg of hyperbranched poly(BAC2-AMPD1)-PEG in 1 mL of DMSO under a rapid stirring. Then the solution was dialyzed using membrane with a molecular weight cut-off of 1000 in deionized water to remove DMSO. In order to investigate pH- and redox-responsive properties, 2 mL of micelle solution was treated using 10 mM hydrochloride or sodium hydroxide solution to designed pH or incubated with 10 mM of GSH at 37 °C under stirring, and the change in the size of the micelles was monitored with dynamic light scattering (DLS).

Preparation of DOX loaded micelles

22.5 mL of deionized water was added at a rate of 0.5 mL/h using a syringe pump to 2.5 mL of DMSO containing 50 mg of hyperbranched poly(BAC2-AMPD1)-PEG, 10 mg of DOX-HCl and 5 µL of triethylamine (TEA) under rapid stirring. Then the solution was dialyzed using membrane with a molecular weight cut-off of 1000 in deionized water to remove DMSO and DOX. After dialysis, aggregates of unloaded DOX were removed by filtration through a filter with a pore diameter of 0.45 µm. To measure the DOX loading capacity, DOX loaded micelle solution was lyophilized, and a certain amount of dried DOX loaded micelles was dissolved in DMSO. The solution was dialyzed using membrane with a molecular weight cut-off of 2000 in DMSO. The concentration of DOX in the dialysis solution was measured with the concentration of DOX being determined based on a calibration curve. The loading capacity and the loading efficiency were calculated:

$$\text{Loading capacity} = \frac{\text{Mass of DOX loaded}}{\text{Mass of DOX loaded micelles}} \times 100\%$$

$$\text{Loading efficiency} = \frac{\text{Mass of DOX loaded}}{\text{Mass of DOX added}} \times 100\%$$

in vitro DOX release profile of DOX loaded micelles

2 mL of the DOX loaded micelle solution in dialysis membrane with a molecular weight cut-off of 10 000 was submerged in 40 mL of phosphate buffered saline (PBS) at 37 °C with various conditions, i.e., pH 7, pH 5, pH 7 with 10 mM of GSH respectively. At a predetermined interval, 4 mL of dialysis solution (PBS) was collected and 4 mL of fresh PBS was added. The fluorescence intensity of the solutions at 590 nm was measured with an excitation of 440 nm, and the concentration of DOX was determined based on a calibration curve.

Preparation of FITC tagged micelles of hyperbranched poly(BAC2-AMPD1)-PEG

The micelle solution was reacted with excess of FITC in the presence of TEA under stirring at room temperature. After 1 day, FITC tagged micelle solution was dialyzed extensively using a membrane a molecular weight cut-off of 1000 in ample of deionized water.

Cellular imaging

MCF-7 and HepG2 cell lines were seeded in 8 chamber borosilicate coverglass with a cell density of 5,000 cells/chamber and were cultured in DMEM supplemented with 10% FBS and 1% penicillin-streptomycin solution in an incubator at 37°C, 5% CO₂, and 95% relative humidity. The cells were allowed to adhere to the chamber bottom upon overnight incubation. Then, the medium was replaced with fresh medium which contained either with or without 0.2 mM of BSO. The cells were incubated for another 3 days before the medium was again replaced with DOX loaded micelles solution or FITC tagged micelle solution in DMEM. At a designed time interval, the medium was removed and the chamber washed with 500 µL of PBS once followed by adding 250 µL of 90 % (v/v) cold ethanol to fix the cells in dark for 10 minutes. After the ethanol was aspirated, the wells were washed with 500 µL of PBS, and 200 µL of 4',6-diamidino-2-phenylindole (DAPI) (10µg/mL) was added to stain the nuclei of the cells. 5 minutes later, DAPI was removed, and the wells were washed with 500 µL of PBS twice followed by adding 150 µL of PBS to prevent the cells from drying up. The cells were imaged under a confocal laser scanning microscope.

Flow cytometry analysis

MCF-7 and HepG2 cell lines were seeded in 12 well-plates with a cell density of 6×10^4 and 3×10^4 cells/chamber respectively and were cultured in DMEM supplemented with 10% FBS and 1% penicillin-streptomycin solution in an incubator at 37°C, 5% CO₂, and 95% relative humidity. The cells were allowed to adhere to the well bottom upon overnight incubation. Then the medium was replaced with fresh medium which contained either with or without 0.2 mM of BSO. The cells were incubated for another 3 days before the medium was again replaced with DOX loaded micelles solution or FITC tagged micelle solution in DMEM. At a designed time interval, the medium was removed and the chamber washed with 500 µL of PBS twice and the cells were unseeded. After centrifugation, the cell pellets were dispersed in 70 % (v/v) ethanol and stored in -20 °C freezer. Lastly, the fixed cell suspensions were analyzed using a flow cytometry analyser.

in vitro cytotoxicity evaluation of samples

in vitro cytotoxicity of hyperbranched poly(BAC2-AMPD1)-PEG, DOX-HCl, and DOX loaded micelles of hyperbranched poly(BAC2-AMPD1)-PEG were evaluated in MCF-7 and HepG2 cell lines. Viability of the cells was assessed by the standard thiazolyl blue [3-(4,5-dimethyliazolyl)-2]-2,5-diphenyl tetrazolium bromide (MTT) assay. This colorimetric assay allows determination of the number of viable cells through the metabolic activity of the cells.

The cancer cells were seeded in 96-well plates with a cell density of 2,500 cells/well and were cultured in DMEM supplemented with 10% FBS and 1% penicillin-streptomycin solution in an incubator at 37 °C, 5% CO₂, and 95% relative humidity. The cells were allowed to adhere to the well bottom

upon overnight incubation. Then, the medium was replaced with fresh medium which contained either with or without 0.2 mM of BSO. The cells were incubated for another 3 days before the medium was exchanged with the sample solutions of different concentrations in DMEM containing with or without 0.2 mM BSO. Meanwhile, wells containing only cell culture medium were prepared as untreated controls. At the predetermined time, the medium containing samples was aspirated and the wells were washed with $1 \times$ PBS solution for two times to removed non-internalized sample. Then 100 µL of DMEM and 10 µL of MTT solution (5 mg/mL in $1 \times$ PBS solution) were added to the wells. After incubation for 4 h at 37 °C, the solution was removed and the formazan precipitate was dissolved in 100 µL of DMSO. The absorbance intensity of the solution was then quantified spectrophotometrically using a microplate reader (TECAN SpectraFluor Plus) at 570 nm. Cell viability was expressed by the following equation:

$$\text{Cell viability (\%)} = \text{Abs sample} / \text{Abs control} \times 100\%$$

Where Abs sample was the absorbance for cells treated with samples, while Abs control was the absorbance for untreated control cells. All the tests were performed in multiples.

Measurements

NMR spectra were obtained on a Bruker DPX 400 MHz NMR spectrometer. A Brookhaven BIS200 laser light scattering system was used for dynamic light scattering (DLS) measurements. The light source is a power adjustable vertically polarized 35 mW argon ion laser with a wavelength of 633 nm. The scattering angle was fixed at 90 ° for measuring the hydrodynamic radius (R_h) and the average scattering intensity. R_h values were obtained using a NNLS analysis. 6 different sample concentrations in methanol were measured at multiple angles, ranging from 50° to 140° to get a Zimm plot. Transmission electron microscopy (TEM) images were obtained using a high resolution Philips CM300 transmission electron microscope (FEGTEM) at 300 kV, and the samples were prepared by dropping micelles solution onto a copper grid covered with carbon followed by drying in a desiccator, and were stained by leaving the dried grids in 1% OsO₄ in heptane for 2 hours followed by drying in desiccator. Fluorescence excitation and emission spectra were recorded on a Perkin-Elmer LS55 Fluorescence Spectroscopy instrument fitted with a R928-sensitive sample photomultiplier. Confocal imaging was done with Olympus Fluoview FV1000 with excitation wavelength of 405 nm while the flow cytometry analysis was done using BD LSR Fortessa Flow Cytometry Analyser.

Results and Discussion

Synthesis of vinyl-terminated hyperbranched poly(BAC2-AMPD1)

Michael Addition polymerization of AMPD with a double molar BAC was conducted in ethanol at 65 °C. Similar to the

Michael addition polymerization of 1-(2-aminoethyl)piperazine (AEPZ) with a double molar of diacrylate,³⁸ the reaction of AMPD with a double molar BAC forms B'B'A intermediate first via the reaction of the 2° amine (original) with BAC as shown in Scheme 1. In Figure 1a, the peaks attributed to B'B'A intermediate appear, e.g., the peak d₂ at ca. 52.9 ppm, after the reaction is performed in ethanol at 65 °C for 0.25 h. At this stage, Figure 1a also shows that unreacted AMPD monomer still exists as reflected by the corresponding peaks, e.g., the peak c₁ at ca. 30.0 ppm. After the reaction was performed for 4 h, Figure 1b shows that B'A₂ intermediate is formed as reflected by the appearance of the corresponding peaks, e.g., the peak a₃ at 55.0 ppm. Vinyl-terminated hyperbranched poly(BAC2-AMPD1) is formed via the polymerization of B'A₂ intermediate. Figure 1c indicates that the dendritic unit is formed as reflected by the appearance of the corresponding peaks, e.g., the peak a₄ at ca. 59.7 ppm, after the reaction is performed for 48 h, with the 2° amine (formed) still existing. Figure 1d indicates that almost all the 2° amine (formed) is consumed as reflected by the disappearance of the corresponding peaks, e.g., the peak a₃, after the reaction is performed for 240 h. Originally, the polymerization was performed in methanol at 50 °C following our previous works,³¹ however, the reaction was slow with the dendritic unit being formed 3 days later, and the 2° amine (formed) being consumed after 28 days. When the polymerization was performed in a mixture of DMSO/water (80/20) (v/v) at 80 °C to increase the reaction rate, no dendritic unit was formed even after 11 days. Therefore, ethanol was adopted for the polymerization.

The vinyl terminal group of hyperbranched poly(BAC2-AMPD1) was converted into amine via the reaction with excess AMPD in DMSO.³⁸ The complete conversion of the vinyl group to amine is indicated by the disappearance of the vinyl peaks at 125.5 ppm and 130.5 ppm as shown in Figure 1e. Three possible reactions may occur between the vinyl group and AMPD as shown in Scheme 1, i.e., the reaction between the vinyl group and 2° amine (original), 1° amine and the cyclic reaction with 2 vinyl terminals, respectively. Since the reactivity sequence of the three amines of AMPD is 2° amine (original) > 1° amine >> 2° amine (formed),^{7,37,40} the vinyl group reacts with the 2° amine (original) instead of 1° amine when excess AMPD is presented. This is supported by the appearance of the characteristic peaks of the unit such as the peak c₂ at 29.4 ppm in Figure 1e. Meanwhile, the peaks attributed to the unit from the reaction with 1° amine such as the peaks a₃ and h₃ cannot be observed. Therefore, most of the vinyl groups react with the 2° amine (original) of AMPD forming hyperbranched poly(BAC2-AMPD1) terminated with -NH₂, hyperbranched poly(BAC2-AMPD1)-NH₂. The molecular weight of hyperbranched poly(BAC2-AMPD1)-NH₂ is determined to be 75.4 ± 1.1 k Dalton from Zimm plot obtained in methanol shown in Figure S1a. Hyperbranched poly(BAC2-AMPD1)-NH₂ is soluble in methanol, ethanol and DMSO, but not in aqueous solution

Figure 1.

Synthesis of hyperbranched poly(BAC2-AMPD1)-PEG

PEG has been demonstrated to have various functions including facilitating membrane penetration⁴²⁻⁴⁷ and endocytosis process,⁴¹ and preventing nonspecific protein adsorption in association with long-circulation time in blood vessel.⁴⁸⁻⁵³ So PEG was conjugated to the -NH₂ terminals of hyperbranched poly(BAC2-AMPD1)-NH₂ via the formation of urethane bond as shown in Scheme 1. To control the degree of PEG conjugation, the feeding molar ratio of PEG to the terminal -NH₂ was kept at 1 : 3.5. From the ¹³C NMR spectrum shown in Figure 1f, the molar ratio of PEG attached is determined to be ca. 1 : 4.1 using equation 1.

$$\text{Molar ratio of PEG / terminals} = 2 \times I_{157.48} / I_{29.29} \quad (1)$$

Where $I_{157.48}$ and $I_{29.4}$ are the integral intensities of the peaks of k and c₂ at 157.5 ppm and 29.4 ppm, respectively.

Hyperbranched poly(BAC2-AMPD1)-PEG is soluble in methanol, ethanol, and DMSO. The molecular weight of hyperbranched poly(BAC2-AMPD1)-PEG is 125.6 ± 2.6 k Dalton obtained from Zimm plot in methanol shown in Figure S1b. So each hyperbranched poly(BAC2-AMPD1) macromolecule is conjugated with ~25 PEG chains determined using equation 2:

$$\text{Number of PEG chains conjugated to each hyperbranched poly(BAC2-AMPD1) macromolecule} = (M_{wB} - M_{wA}) / 2000 \quad (2)$$

Where M_{wB} and M_{wA} are the molecular weights of hyperbranched poly(BAC2-AMPD1)-PEG and hyperbranched poly(BAC2-AMPD1)-NH₂, respectively.

Self-assembly of hyperbranched poly(BAC2-AMPD1)-PEG

Polymer self-assembly occurred when deionized water was added at a rate of 0.5 ml/h into DMSO solution of hyperbranched poly(BAC2-AMPD1)-PEG. Figure 2a presents TEM images of the self-assembly obtained stained with OsO₄. It can be observed that the self-assembly is in the form of micelles with an average diameter of ca. 87 nm at dry state. DLS measurements show that the diameter of the swollen micelles obtained in aqueous solution is ca. 233.2 ± 13.4 nm. The critical micelle concentration (CMC) of the micelles was determined to be ca. 21.1 µg/mL by using DLS to plot the average scattering intensities of different polymer concentrations as shown in Figure S2b.^{7,54} Since only the protons of polymer segments with a high mobility in solution can be observed in solution ¹H NMR spectrum,⁵⁵⁻⁵⁷ ¹H NMR spectra were used to get more information of the micelles formed. Figures 3a and 3b show ¹H NMR spectra of hyperbranched poly(BAC2-AMPD1)-PEG in methanol-d₄ and in deuterium oxide (D₂O) obtained by dissolving directly, respectively. Although the peaks become broadened, most of the peaks in Figure 3a can still be observed in Figure 3b. Figure

3c shows ^1H NMR spectrum of micelles obtained by adding D_2O slowly into DMSO solution of hyperbranched poly(BAC2-AMPD1)-PEG followed by dialysis. In comparison with Figure 3b, it is obvious that only the peaks attributed to PEG can be observed which indicates that the micelles are formed with PEG shells and poly(BAC2-AMPD1) cores inaccessible to water.^{7,55-57} So the micelles can only be obtained via slow addition of water into DMSO solution of hyperbranched poly(BAC2-AMPD1)-PEG rather than dissolving in water directly. The self-assembly of hyperbranched poly(BAC2-AMPD1)-PEG is facilitated by a gradient change from a good solvent for both the hydrophilic and hydrophobic components to a selective solvent only for the hydrophilic component.

Figures 2 and 3.

pH dependent hydrodynamic diameter of the micelles of hyperbranched poly(BAC2-AMPD1)-PEG was investigated using DLS (the results shown in Figure S3a). As pH was decreased, the diameter of the micelles increased due to swelling induced by the protonation of the amines. Also it was shown that the average scattering intensity of the micelles declined by more than 95% in 15 minutes after incubation with 10 mM of GSH (See Figure S4) which indicates that the micelles can be degraded via the reaction with GSH.

DOX loaded micelles of hyperbranched poly(BAC2-AMPD1)-PEG

Anti-cancer drug, DOX which intercalate with DNA to induce cell death,^{58,59} was loaded into the micelles of hyperbranched poly(BAC2-AMPD1)-PEG during the self-assembly process. DOX content and loading efficiency of the micelles of hyperbranched poly(BAC2-AMPD1)-PEG are ca. 10.5 % and ca. 52.3 %, respectively. DOX loaded micelles have a hydrodynamic diameter of ca. 193.1 ± 17.65 nm determined using DLS, and a diameter of ca. 108 nm in dry state obtained from TEM image as shown Figure 2b. CMC of DOX loaded micelles is 4.5 $\mu\text{g}/\text{ml}$, which is lower than the micelles without DOX (illustrated in Figure S2c).

The release profiles of DOX from micelles of hyperbranched poly(BAC2-AMPD1)-PEG were investigated in PBS under pH 7, pH 5, and pH 7 with 10 mM GSH, respectively, and the results are shown in Figure 4. The release rate of DOX is considerably faster at pH 5 than at pH 7. After 10 h, 17 % of DOX is released at pH 7 as compared to 35% at pH 5. A lower pH leads to a higher protonation degree of the amines of poly(BAC2-AMPD1) associated with a greater swelling of the micelles and therefore a faster release of DOX. When the DOX loaded micelle solution is incubated with 10 mM of GSH, a much faster release is observed with 50 % and 100% of DOX being released in 10 h and 72 h, respectively. This is caused by thiol-induced degradation leading to dissociation of the micelles.

Figure 4.

Cellular uptake of FITC tagged micelles and DOX loaded micelles

The cellular uptake of the micelles of hyperbranched poly(BAC2-AMPD1)-PEG was investigated using confocal microscopy. Although fluorescence can be observed from poly(amido amine)s similar to those amine-containing polymers,⁶⁰ the micelles were tagged with FITC for accurate analysis. FITC tagged micelles were incubated with HepG2 and MCF-7 cells for 72 h. Both HepG2 and MCF-7 cells, with a high intracellular GSH level, were also incubated with 0.2 mM of BSO for 72 h to reduce the intracellular GSH concentration by ca. 4 times in order to investigate the effects of reductive potential.¹⁷ Figure 5 shows the confocal microscopy images of HepG2 cells after incubation with FITC tagged micelles of hyperbranched poly(BAC2-AMPD1)-PEG for different time intervals. In HepG2 without or with BSO treatment, FITC fluorescence is detected in the cytoplasm after incubation for 5 h. This indicates that FITC tagged micelles can enter the cells readily probably via endocytosis. The effect of BSO treatment on the HepG2 is indicated by the results of flow cytometry shown in Figure 6. BSO treatment results in higher fluorescence intensity from HepG2, and the fluorescence intensity increases with the incubation time from 5 h to 72 h. In contrast, the fluorescence intensity from the cells without BSO treatment increases by ca. 40% as the incubation time increases from 5 h to 24 h, and then drops ca. 12% after 72h incubation. This might be due to that a lower reduction potential in the intracellular apartments induced by BSO treatment retards the degradation of the micelles, and therefore leads to accumulation of more FITC tagged micelles in the cytoplasm.

Figures 5 and 6.

Figure 7 shows the confocal microscopy images of MCF-7 cells after incubation with FITC tagged micelles of hyperbranched poly(BAC2-AMPD1)-PEG. Similarly the micelles can enter the cells readily without or with BSO treatment. The flow cytometry results shown in Figure 8 indicates that the fluorescence intensity reaches the maximum at 24 h and then decreases with time, and the effect of BSO treatment on MCF-7 cells is a negligible, which is similar to the phenomenon reported.¹⁷

Figures 7 and 8.

DOX loaded micelles of hyperbranched poly(BAC2-AMPD1)-PEG were incubated with HepG2 and MCF-7 cells without or with BSO treatment, respectively. As shown in Figure 5 and 7, DOX can be observed in the cytoplasm and nucleus of HepG2 and MCF-7 cells after incubation of 5 h. The results from flow cytometry in Figure 6 shows that DOX fluorescence intensity increase insignificantly with incubation time from 5 h to 72 h in HepG2 cells; and increase from 5 h to 24 h but level off till 72 h in MCF-7 cells. The effect of BSO

treatment is negligible on the DOX fluorescence intensity in both HepG2 and MCF-7 cells.

in vitro cytotoxicity of DOX loaded micelles

in vitro cytotoxicity of hyperbranched poly(BAC2-AMPD1)-PEG and DOX loaded micelles were evaluated in HepG2 and MCF-7 without or with BSO treatment, respectively. More than 70 % of the HepG2 cells and MCF-7 cells are viable after incubation with 200 µg/ml of hyperbranched poly(BAC2-AMPD1)-PEG for 72 h regardless of without or with BSO treatment, which shows a low cytotoxicity of the polymer (shown in Figure S5). Figures 9 and 10 illustrate the cytotoxicity of DOX loaded micelles of hyperbranched poly(BAC2-AMPD1)-PEG in HepG2 cells and MCF-7 cells, respectively. Figure 9 indicates that free DOX-HCl displays a higher cytotoxicity than DOX loaded micelles in HepG2 cells without or with BSO treatment. Furthermore, it is also reflected that BSO treatment shows insignificant effects on the cytotoxicity of free DOX-HCl and DOX loaded micelles of hyperbranched poly(BAC2-AMPD1)-PEG. Figure 10 shows that DOX loaded micelles of hyperbranched poly(BAC2-AMPD1)-PEG shows cytotoxicity comparable to free DOX-HCl in MCF-7 cells without or with BSO treatment, and the effects of BSO treatment is also insignificant. Since the DOX loaded micelles can release all the DOX loaded in 72 h at pH 7 with 10 mM GSH as shown in Figure 4, the difference in cytotoxicity of DOX loaded micelles and free DOX-HCl in HepG2 and MCF-7 cells should not be due to the incomplete release of DOX, and should be attributed to the different cell endocytosis process instead. So far, the cell endocytosis is still not well understood. Many features of nanoparticles including shape, size, and surface properties affect the cellular uptake,^{61,62} and endocytosis process is also cell type dependent and has many internalization routes such as clathrin-coated pit-mediated endocytosis and raft mediated endocytosis.⁶¹⁻⁶³

Figures 9 and 10.

Conclusions

Vinyl terminated hyperbranched poly(amido amine)s is synthesized via Michael Addition polymerization of -AMPD with a double molar BAC in ethanol. After the terminal vinyl groups is converted to primary amines via reaction with excess AMPD, PEG is conjugated to form hyperbranched poly(BAC2-AMPD1)-PEG. pH- and redox-responsive micelles with PEG shells and hydrophobic cores of poly(BAC2-AMPD1) can be formed via self-assembly of hyperbranched poly(BAC2-AMPD1)-PEG in aqueous solution, and DOX can be loaded within the micelles with loading capacity and efficiency of ca. 10.5 % and ca. 52.3 % respectively. DOX can be released faster at pH 5 and in the presence of 10 mM of GSH. The micelles of hyperbranched poly(BAC2-AMPD1)-PEG without or with DOX can enter HepG2 and MCF-7 cells readily, and DOX can be observed in the nucleus of the cells. DOX loaded micelles of

hyperbranched poly(BAC2-AMPD1)-PEG can kill HepG2 and MCF-7 cells with the cytotoxicity lower or close to free DOX-HCl. A lower reductive potential induced by BSO treatment shows insignificant effects on these performances, except in HepG2 where it was shown that more micelles can accumulated in cells with lower intracellular reductive potential.

Acknowledgements

The financial support is from A*Star under JCO programme, JCO DP programme, Biomass programme and Personal Care programme.

Notes

^a Institute of Materials Research and Engineering, A*STAR (Agency for Science, Technology and Research), 3 Research Link, 117602, Singapore. E-mail: ye-liu@imre.a-star.edu.sg

^b Department of Bioengineering, National University of Singapore, 9 Engineering Drive 1, Block EA #03-12, 117575, Singapore.

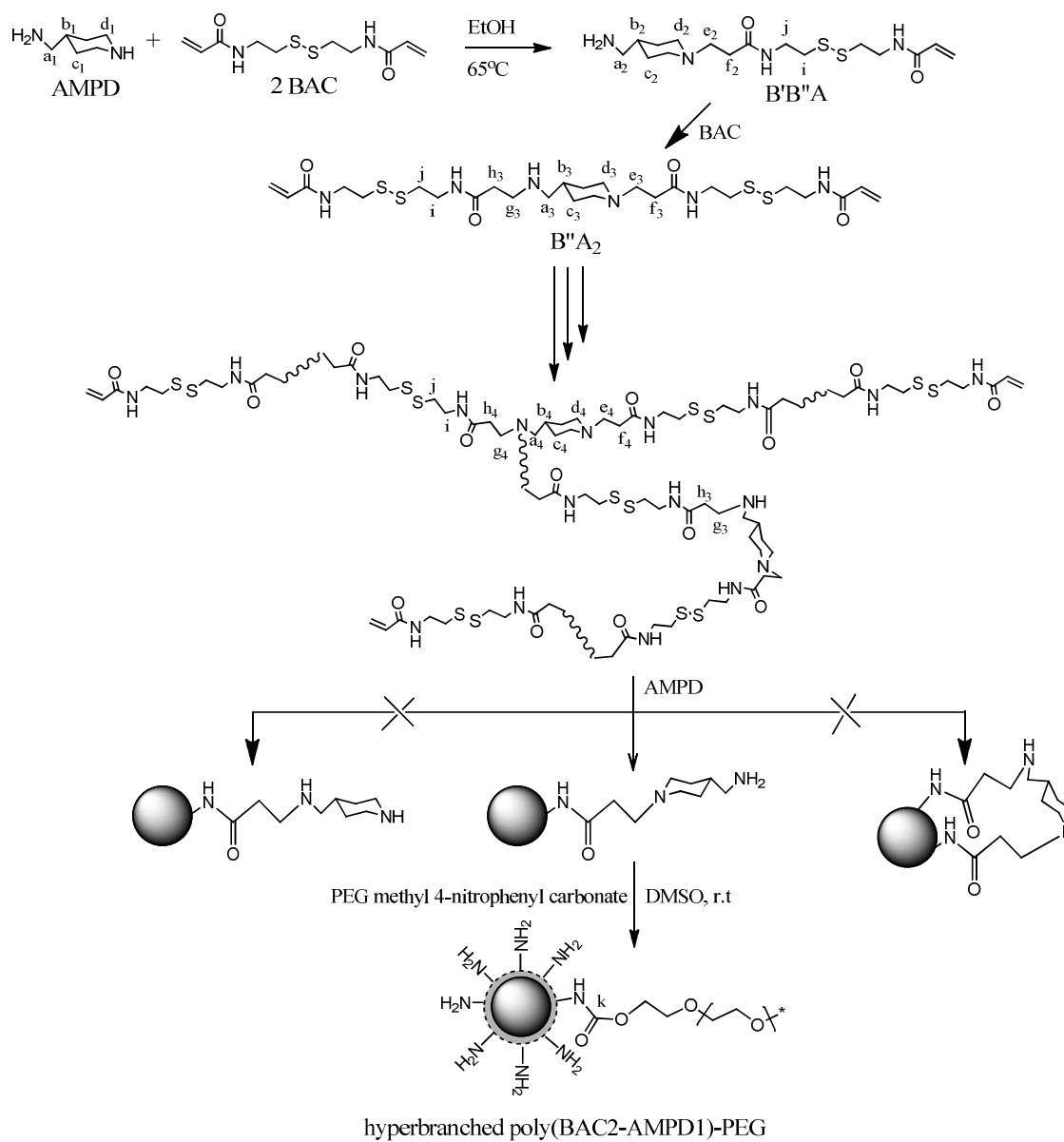
References

- a) S. Mura, J. Nicolas, P. Couvreur, *Nat. Mater.*, **2013**, *12*, 991-1003.
b) W. Cheng, L. Gu, W. Ren, Y. Liu, *Mater. Sci. Eng.: C.*, **2014**, DOI: 10.1016/j.msec.2014.05.050.
- R. A. Cairns, I. S. Harris, T. W. Mak, *Nat. Rev. Cancer*, **2011**, *11*, 85-95.
- F. Q. Schafer, G. R. Buettner, *Free Radic. Biol. Med.*, **2001**, *30*, 1191-1212.
- A. A. Stavrovskaya, *Biochemistry (Moscow)*, **2000**, *65*, 95-106.
- J. Yao, Y. Ruan, T. Zhai, J. Guan, G. Tang, H. Li, S. Dai, *Polymer*, **2011**, *52*, 3396-3404.
- Y. Y. Li, S. H. Hua, W. Xiao, H. Y. Wang, X. H. Luo, C. Li, S. X. Cheng, X. Z. Zhang, R. X. Zhuo, *J. Mater. Chem.*, **2011**, *21*, 3100-3106.
- W. Cheng, J. N. Kumar, Y. Zhang, Y. Liu, *Macromol. Biosci.*, **2014**, *14*, 347-358.
- R. P. Johnson, Y. I. Jeong, E. Choi, C. W. Chung, D. H. Kang, S. O. Oh, H. Suh, I. Kim, *Adv. Funct. Mater.*, **2012**, *22*, 1058-1068.
- G. Chang, C. Li, W. Lu, J. Ding, *Macromol. Biosci.*, **2010**, *10*, 1248-1256.
- E. S. Lee, K. T. Oh, D. Kim, Y. S. Youn, Y. H. Bae, *J. Control. Release*, **2007**, *123*, 19-26.
- E. R. Gillies, A. P. Goodwin, J. M. J. Fréchet, *Bioconjugate Chem.*, **2004**, *15*, 1254-1263.
- A. Ponta, Y. Bae, *Pharm. Res.*, **2010**, *27*, 2330-2342.
- H. J. Lee, Y. Bae, *Pharm. Res.*, **2013**, *30*, 2077-2086.
- S. Akter, B. F. Clem, H. J. Lee, J. Chesney, Y. Bae, *Pharm. Res.*, **2012**, *29*, 847-855.
- Y. Bae, S. Fukushima, A. Harada, K. Kataoka, *Angew. Chem. Int. Ed.*, **2003**, *42*, 4640-4643.
- M. D. Howard, A. Ponta, A. Eckman, M. Jay, Y. Bae, *Pharm. Res.*, **2011**, *28*, 2435-2446.
- Y. Ping, D. Wu, J. N. Kumar, W. Cheng, C. L. Lay, Y. Liu, *Biomacromolecules*, **2013**, *14*, 2083-2094.

- 18 a) A. N. Koo, K. H. Min, H. J. Lee, S. U. Lee, K. Kim, I. Chan Kwon, S. H. Cho, S. Y. Jeong, S. C. Lee, *Biomaterials*, **2012**, *33*, 1489-1499. b) F. Meng, W. E. Hennink, Z. Zhong, *Biomaterials*, **2009**, *30*, 2180-2198.
- 19 M. Calderón, R. Graeser, F. Kratz, R. Haag, *Bioorg. Med. Chem. Lett.*, **2009**, *19*, 3725-3728.
- 20 J. Liu, W. Huang, Y. Pang, X. Zhu, Y. Zhou, D. Yan, *Biomacromolecules*, **2010**, *11*, 1564-1570.
- 21 R. Haag, F. Kratz, *Angew. Chem. Int. Ed.*, **2006**, *45*, 1198-1215.
- 22 X. Huang, G. Song, S. Yu, I. Kim, *J. Mater. Sci.*, **2013**, *48*, 5163-5170.
- 23 P. Kolhe, E. Misra, R. M. Kannan, S. Kannan, M. Lieh-Lai, *Int. J. Pharm.*, **2003**, *259*, 143-160.
- 24 S. Kannan, P. Kolhe, V. Raykova, M. Glibatec, R. M. Kannan, M. Lieh-Lai, D. Bassett, *J. Biomater. Sci. Polym. Ed.*, **2004**, *15*, 311-330.
- 25 H. Zhang, C. Zhao, H. Cao, G. Wang, L. Song, G. Niu, H. Yang, J. Ma, S. Zhu, *Biomaterials*, **2010**, *31*, 5445-5454.
- 26 R. B. Arote, H. L. Jiang, Y. K. Kim, M. H. Cho, Y. J. Choi, C. S. Cho, *Expert Opin. Drug Deliv.*, **2011**, *8*, 1237-1246.
- 27 L. V. Christensen, C. W. Chang, J. K. Won, W. K. Sung, Z. Zhong, C. Lin, J. F. J. Engbersen, J. Feijen, *Bioconjugate Chem.*, **2006**, *17*, 1233-1240.
- 28 X. Wang, Y. He, J. Wu, C. Gao, Y. Xu, *Biomacromolecules*, **2010**, *11*, 245-251.
- 29 R. Wang, L. Zhou, Y. Zhou, G. Li, X. Zhu, H. Gu, X. Jiang, H. Li, J. Wu, L. He, X. Guo, B. Zhu, D. Yan, *Biomacromolecules*, **2010**, *11*, 489-495.
- 30 P. Ferruti, M. A. Marchisio, R. Duncan, *Macromol. Rapid Commun.*, **2002**, *23*, 332-355.
- 31 D. Wu, X. J. Loh, Y. L. Wu, C. L. Lay, Y. Liu, *J. Am. Chem. Soc.*, **2010**, *132*, 15140-15143.
- 32 H. Sun, B. Guo, R. Cheng, F. Meng, H. Liu, Z. Zhong, *Biomaterials*, **2009**, *30*, 6358-6366.
- 33 W. Cheng, R. Rajendran, W. Ren, L. Gu, Y. Zhang, K. H. Chuang, Y. Liu, *J. Mater. Chem. B*, **2014**, *2*, 5295-5301.
- 34 E. Emilriti, E. Ranucci, P. Ferruti, *J. Polym Sci Part A*, **2005**, *43*, 1404-1416.
- 35 D. Wang, Y. Liu, Z. Hu, C. Hong, C. Pan, *Polymer*, **2005**, *46*, 3507-3514.
- 36 D. Wu, Y. Liu, X. Jiang, L. Chen, C. He, S. H. Goh, K. W. Leong, *Biomacromolecules*, **2005**, *6*, 3166-3173.
- 37 D. Wu, Y. Liu, C. He, T. Chung, S. Goh, *Macromolecules*, **2004**, *37*, 6763-6770.
- 38 D. Wu, Y. Liu, L. Chen, C. He, T. S. Chung, and S. H. Goh, *Macromolecules*, **2005**, *38*, 5519-5525.
- 39 Y. Liu, D. Wu, Y. Ma, G. Tang, S. Wang, C. He, T. Chung, S. Goh, *Chem. Commun.*, **2003**, *9*, 2630-2631.
- 40 W. Cheng, G. Wang, X. Pan, Y. Zhang, B. Z. Tang, Y. Liu, *Macromol. Biosci.*, **2014**, DOI: 10.1002/mabi.201400076.
- 41 C. L. Lay, H. Q. Liu, D. Wu, Y. Liu, *Chem. Eur. J.*, **2010**, *16*, 3001-3004.
- 42 S. K. Lai, D. E. O'Hanlon, S. Harrold, S. T. Man, Y. Y. Wang, R. Cone, J. Hanes, *Proc. Nat. Academy Sci. U. S. A.*, **2007**, *104*, 1482-1487.
- 43 S. K. Lai, Y. Y. Wang, J. Hanes, *Advanced Drug Delivery Rev.* **2009**, *61*, 158-171.
- 44 Y. Cu, W. M. Saltzman, *Mol. Pharm.*, **2009**, *6*, 173-181.
- 45 J. S. Suk, S. K. Lai, Y. Y. Wang, L. M. Ensign, P. L. Zeitlin, M. P. Boyle, J. Hanes, *Biomaterials*, **2009**, *30*, 2591-2597.
- 46 B. C. Tang, M. Dawson, S. K. Lai, Y. Y. Wang, J. S. Suk, M. Yang, P. Zeitlin, M. P. Boyle, J. Fu, J. Hanes, *Proc. Nat. Academy Sci. U. S. A.*, **2009**, *106*, 19268-19273.
- 47 Y. Y. Wang, S. K. Lai, J. S. Suk, A. Pace, R. Cone, J. Hanes, *Angew. Chem. Int. Ed.*, **2008**, *47*, 9726-9729.
- 48 D. D. Lasic, D. Papahadjopoulos, *Medical Applications of Liposomes, Elsevier Science, Amsterdam*, **1998**.
- 49 J. C. M. Lee, H. Bermudez, B. M. Discher, M. A. Sheehan, Y. Y. Won, F. S. Bates, D. E. Discher, *Biotechnol. Bioeng.*, **2001**, *73*, 135-145.
- 50 M. Antonietti, S. Forster, *Advanced Mater.*, **2003**, *15*, 1323-1333.
- 51 D. E. Discher, A. Eisenberg, *Science*, **2002**, *297*, 967-973.
- 52 V. P. Torchilin, *Nat. Rev. Drug Discov.*, **2005**, *4*, 145-160.
- 53 G. Prencipe, S. M. Tabakman, K. Welsher, Z. Liu, A. P. Goodwin, L. Zhang, J. Henry, H. J. Dai, *J. Am. Chem. Soc.*, **2009**, *131*, 4783-4787.
- 54 H. Hussain, B. H. Tan, C. S. Gudipati, C. B. He, Y. Liu, T. P. Davis, *Langmuir*, **2009**, *25*, 5557-5564.
- 55 J. V. M. Weaver, Y. Tang, S. Liu, P. D. Iddon, R. Grigg, N. C. Billingham, S. P. Armes, R. Hunter, S. P. Rannard, *Angew. Chem. Int. Ed.*, **2004**, *43*, 1389-1392.
- 56 Y. Li, B. S. Lokitz, C. L. McCormick, *Angew. Chem. Int. Ed.*, **2006**, *45*, 5792-5795.
- 57 C. L. Lay, H. R. Tan, X. Lu, Y. Liu, *Chem. Eur. J.*, **2011**, *17*, 2504-2509.
- 58 H. Carvalho, L. M. Garrido, R. L. A. Furlan, G. Padilla, M. Agnoletto, T. Guecheva, J. A. P. Henriques, J. Saffi, C. F. M. Menck, *Cancer Chemother. Pharmacol.*, **2010**, *65*, 989-994.
- 59 G. P. Sartiano, W. E. Lynch, D. Bullington, *J. Antibiotics*, **1979**, *32*, 1038-1045.
- 60 X. Pan, G. Wang, C. L. Lay, B. H. Tan, C. He, Y. Liu, *Sci. Rep.*, **2013**, *3*, DOI: 10.1038/srep02763.
- 61 T. G. Iversen, T. Skotland, K. Sandvig, *Nano Today*, **2011**, *6*, 176-185.
- 62 R. A. Petros, J. M. DeSimone, *Nat. Rev. Drug Discov.*, **2010**, *9*, 615-627.
- 63 L. Rajendran, H. J. Knolker, K. Simons, *Nat. Rev. Drug Discov.*, **2010**, *9*, 29-42.

FIGURES AND SCHEMES

Scheme 1. Synthesis of hyperbranched poly(BAC2-AMPD1)-PEG.



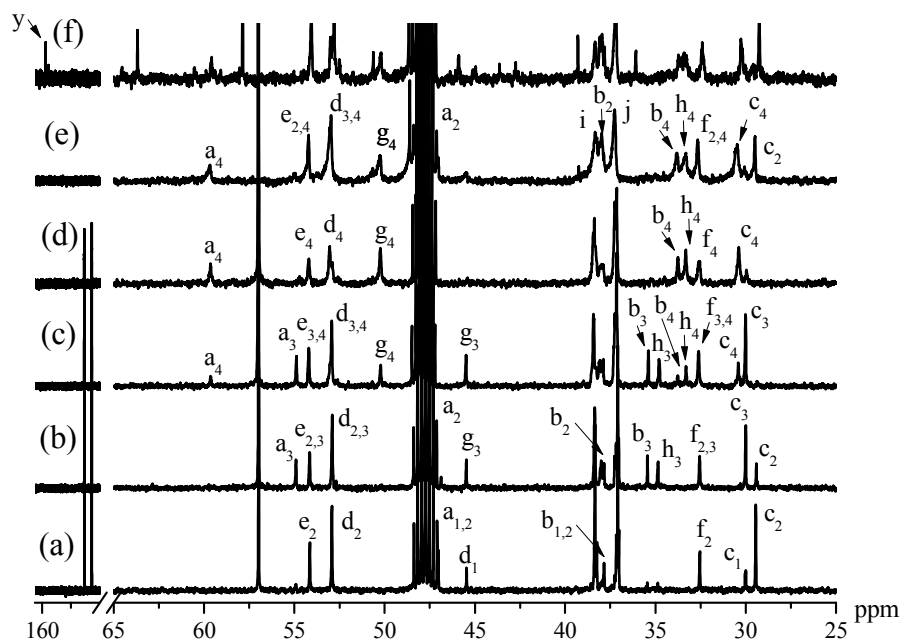


Figure 1. Comparison of ^{13}C NMR spectra of the product of Michael Addition polymerization of AMPD with a double molar BAC in ethanol with a monomer concentration of 25% (w/v) at 65 °C obtained a) for 0.25 h; b) for 4 h; c) for 48 h; d) for 240 h; e) after reaction with AMPD, and f) after PEGylation. The spectra were obtained in methanol- d_4 . The attribution of the peaks is listed in Scheme 1. The peak at 57.0 ppm is attributed to residual ethanol.

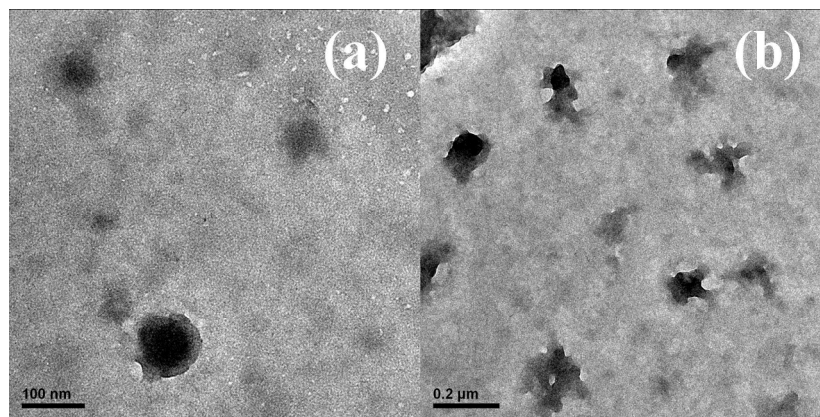


Figure 2. TEM images of a) micelles of hyperbranched poly(BAC2-AMPD1)-PEG stained with osmium (VIII) oxide; b) DOX loaded micelles of hyperbranched poly(BAC2-AMPD1)-PEG stained with osmium (VIII) oxide.

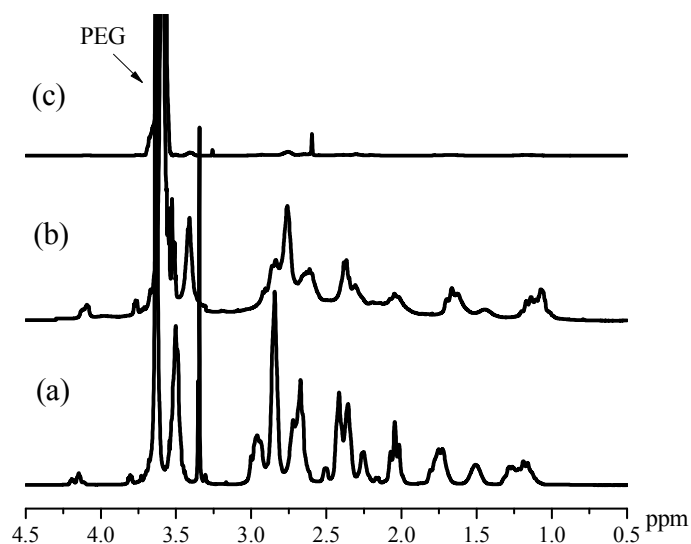


Figure 3. ¹H NMR spectra of a) hyperbranched poly(BAC2-AMPD1)-PEG in methanol-d₄; b) hyperbranched poly(BAC2-AMPD1)-PEG dissolved in D₂O directly; c) micelles of hyperbranched poly(BAC2-AMPD1)-PEG in D₂O, formed by adding D₂O into DMSO followed by dialysis.

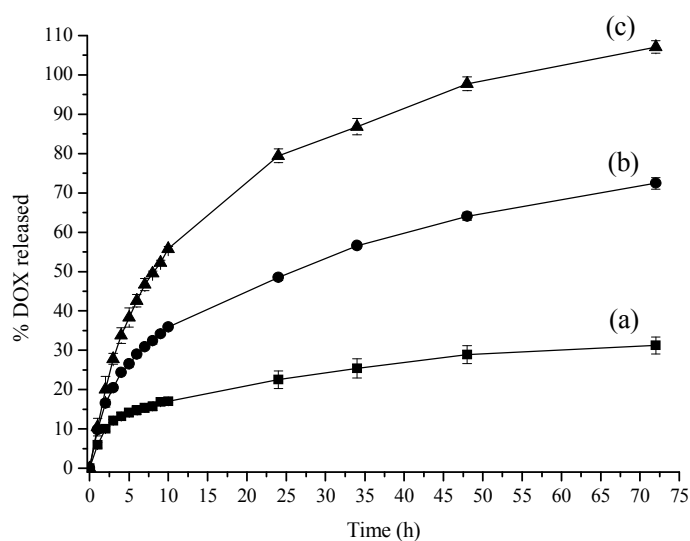


Figure 4. Release profiles of DOX from micelles of hyperbranched poly(BAC2-AMPD1)-PEG at (a) pH 7; (b) pH 5; (c) pH 7 with 10 mM GSH. All data represent mean \pm SD ($n = 3$).

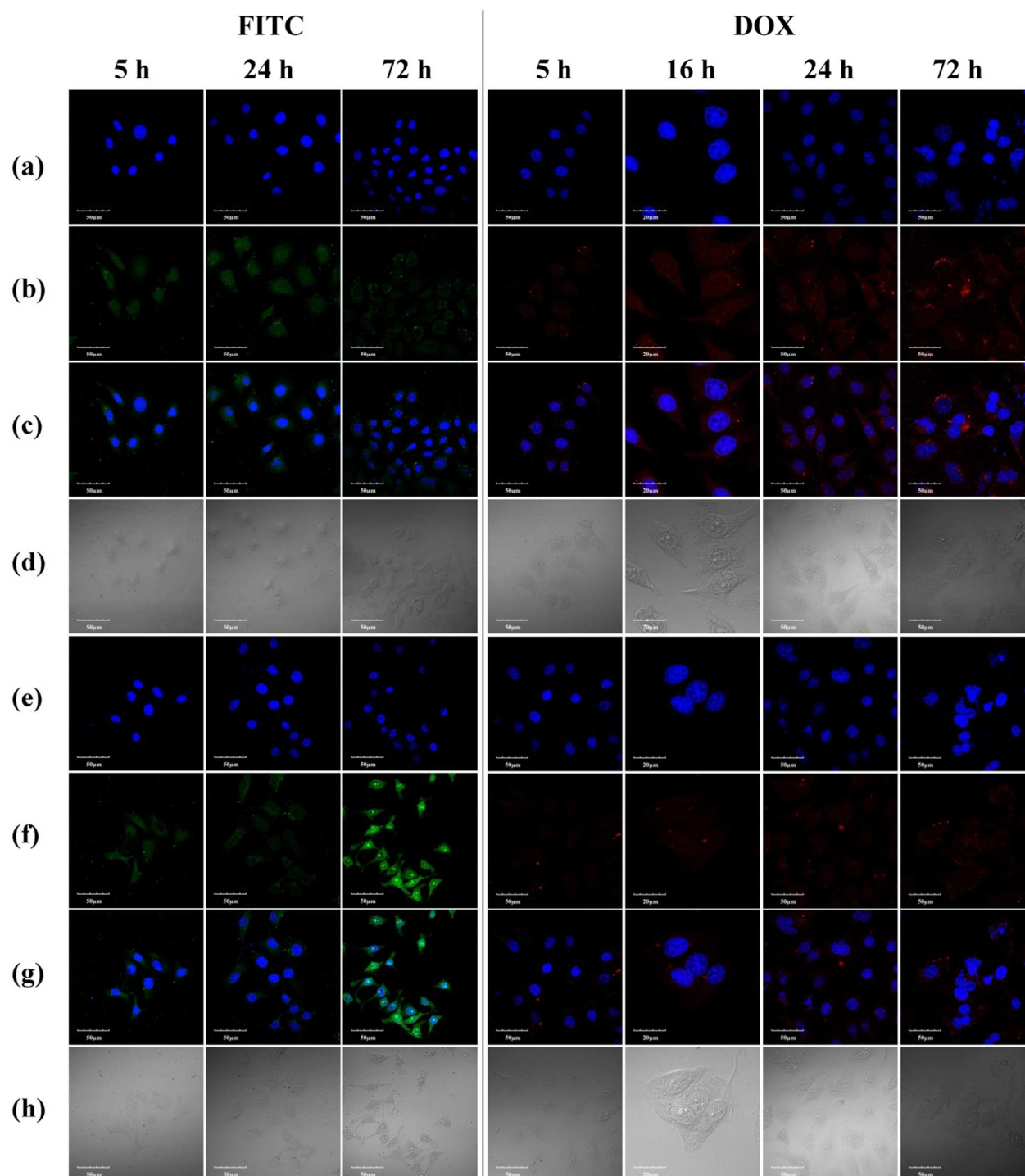


Figure 5. CLSM images of HepG2 cells incubated with FITC tagged micelles of hyperbranched poly(BAC2-AMPD1)-PEG and DOX loaded micelles of hyperbranched poly(BAC2-AMPD1)-PEG. a,e) cells with nucleus staining with DAPI; b,f) cells with FITC or DOX fluorescence; c,g) overlays of cells with nucleus staining with DAPI and FITC or DOX fluorescence; d,h) under bright field. Row (a-d) and (e-h) are results without and with BSO treatment, respectively.

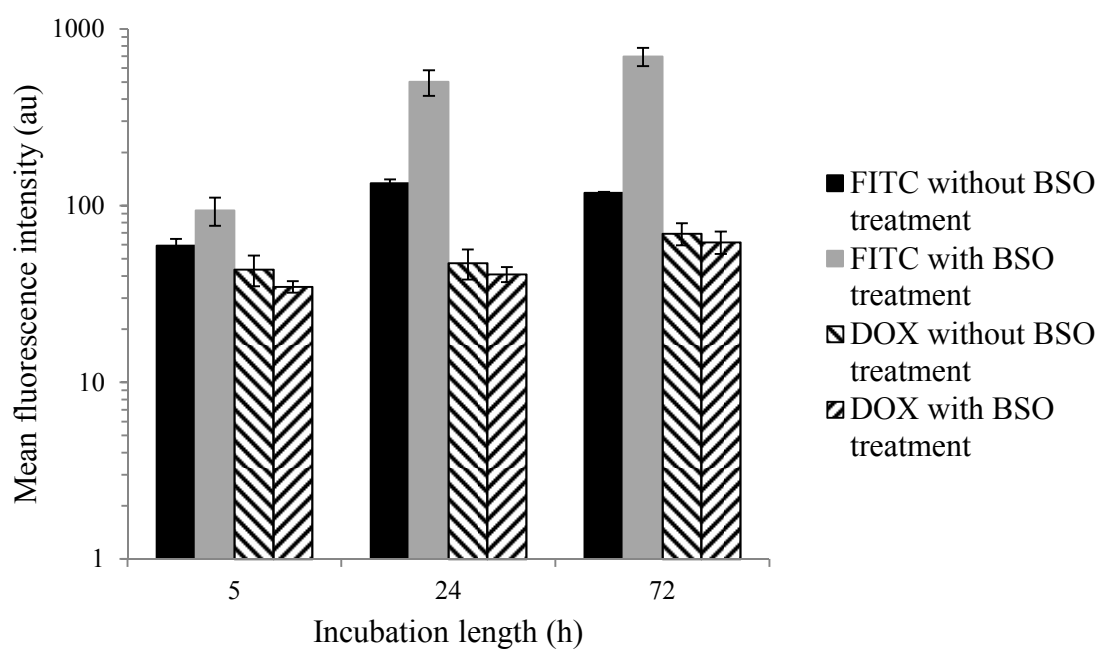


Figure 6. Mean FITC and DOX fluorescence intensity obtained using flow cytometry after HepG2 cells were incubated with FITC tagged micelles of hyperbranched poly(BAC2-AMPD1) and DOX loaded micelles of hyperbranched poly(BAC2-AMPD1) for different time, respectively. All data represent mean \pm SD. (n = 3).

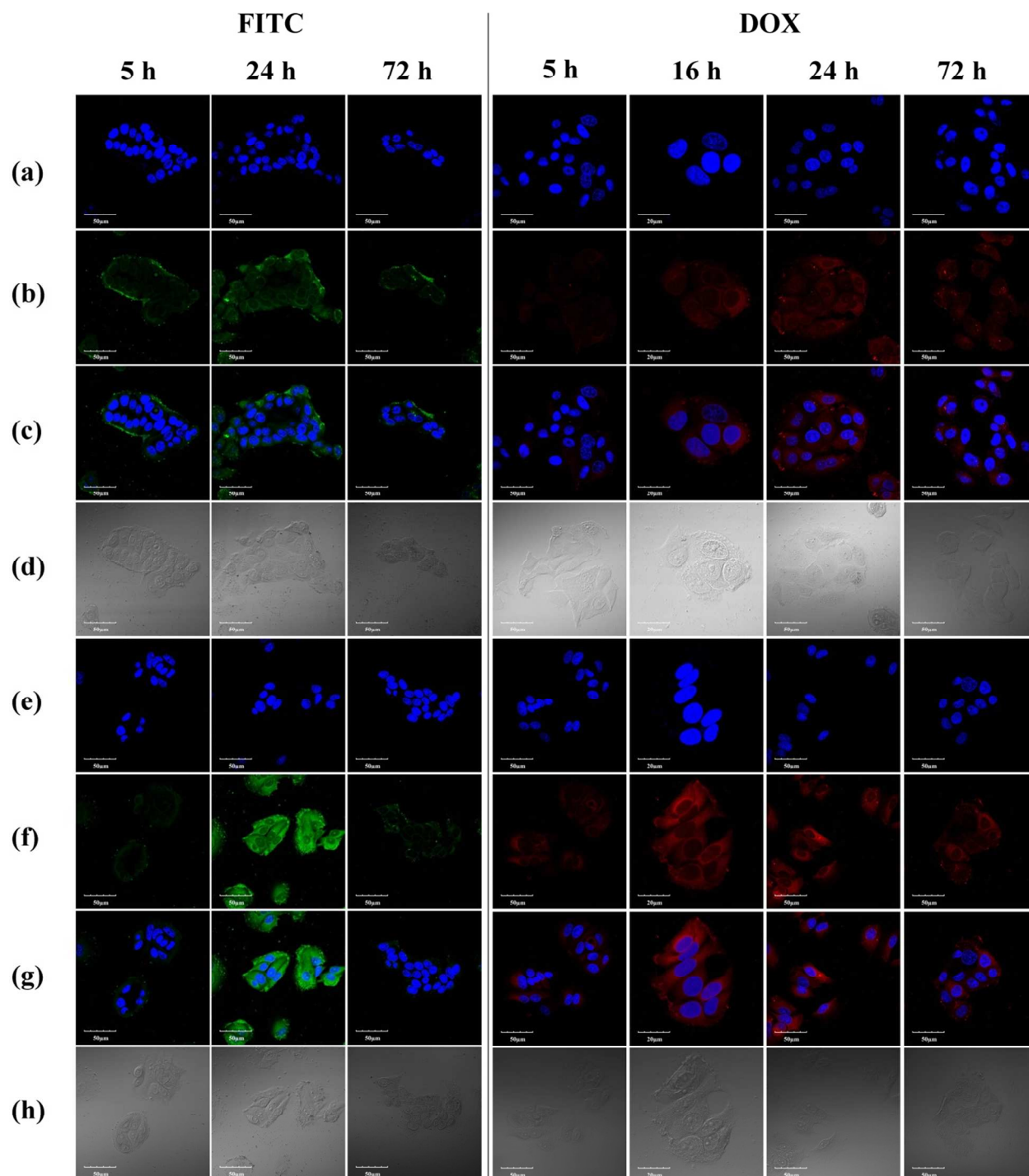


Figure 7. CLSM images of MCF-7 cells incubated with FITC tagged micelles of hyperbranched poly(BAC2-AMPD1)-PEG and DOX loaded micelles of hyperbranched poly(BAC2-AMPD1)-PEG. a,e) cells with nucleus staining with DAPI; b,f) cells with FITC or DOX fluorescence; c,g) overlays of cells with nucleus staining with DAPI and FITC or DOX fluorescence; d,h) under bright field. Row (a-d) and (e-h) are results without and with BSO treatment, respectively.

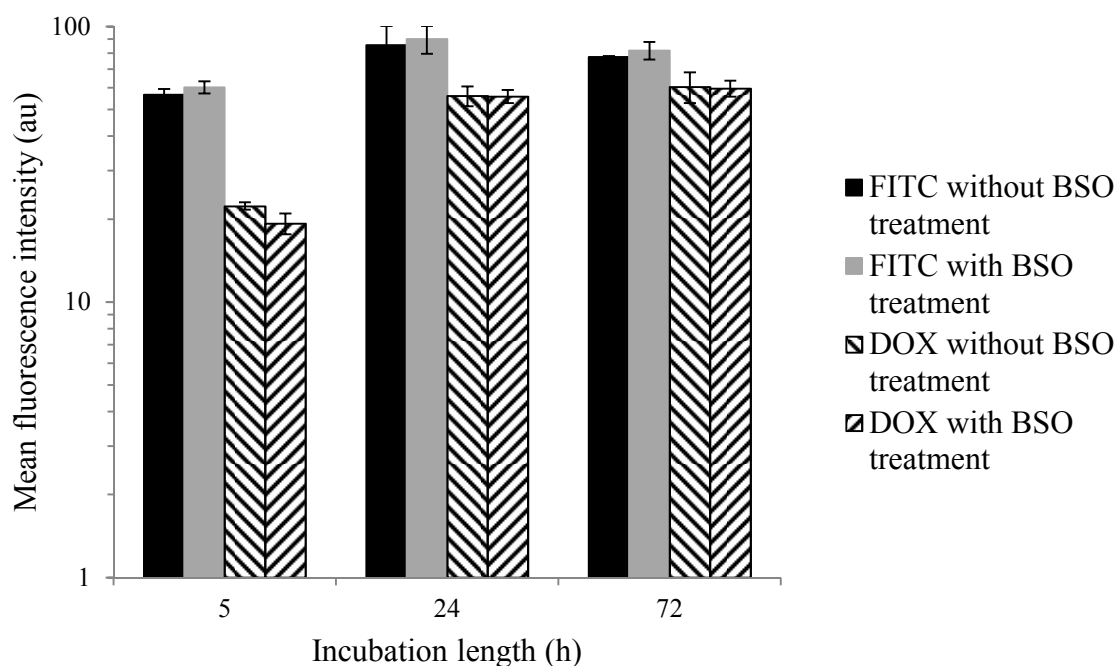


Figure 8. Mean FITC and DOX fluorescence intensity obtained using flow cytometry after MCF-7 cells were incubated with FITC tagged micelles of hyperbranched poly(BAC2-AMPD1) and DOX loaded micelles of hyperbranched poly(BAC2-AMPD1) respectively. All data represent mean \pm SD. (n = 3).

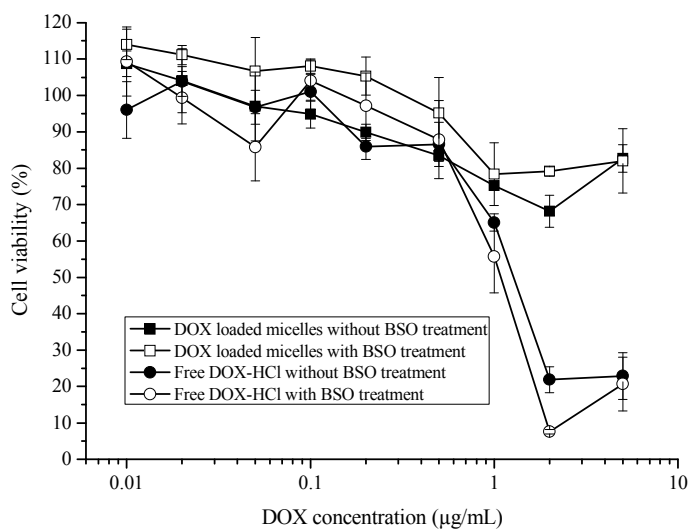


Figure 9. *in vitro* cytotoxicity of DOX loaded micelles of hyperbranched poly(BAC2-AMPD1)-PEG and free DOX-HCl in HepG2 without or with BSO treatment. All data represent mean \pm SD. (n = 3).

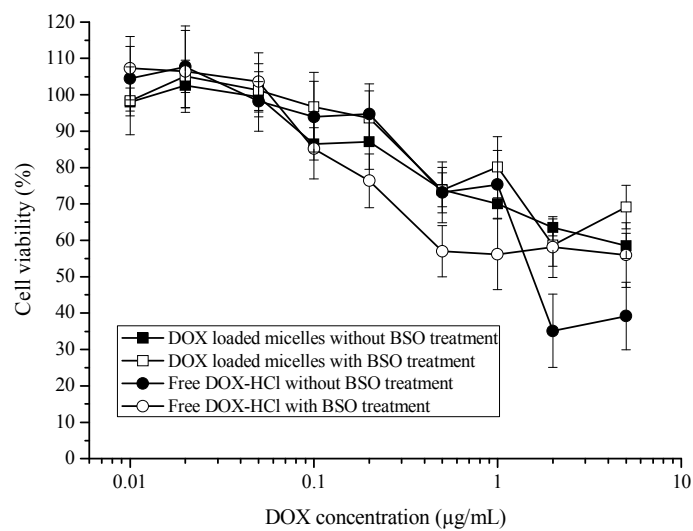
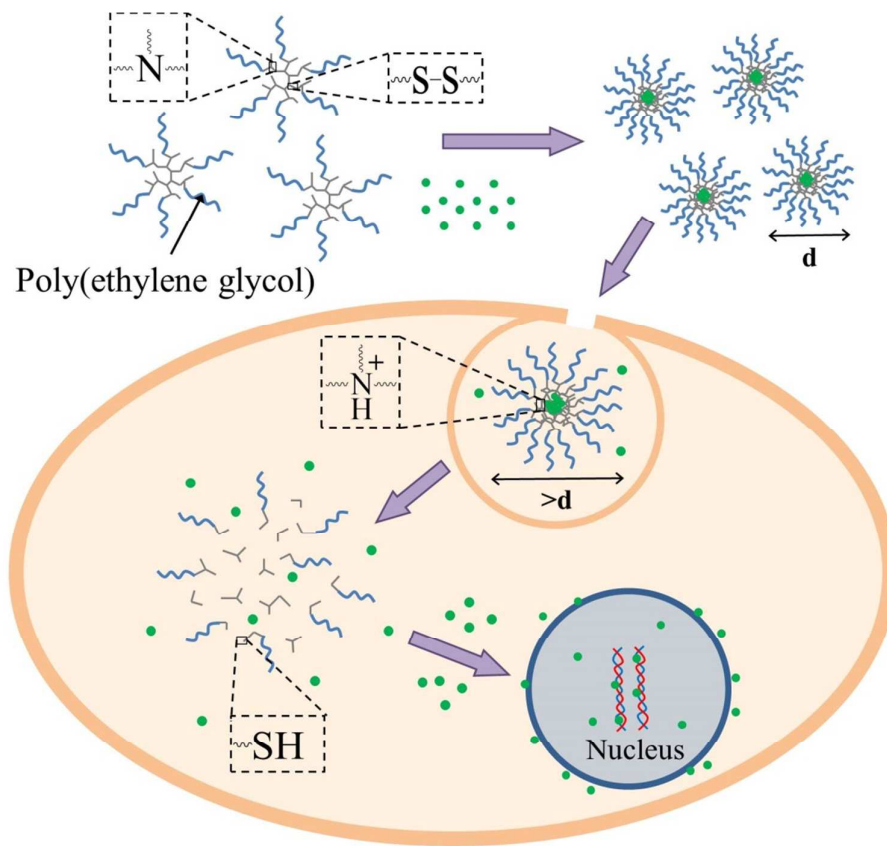


Figure 10. *in vitro* cytotoxicity of DOX loaded micelles of hyperbranched poly(BAC2-AMPD1)-PEG and free DOX-HCl in MCF-7 without or with BSO treatment. All data represent mean \pm SD. (n = 3).

Graphical Abstract



Micelles formed from self-assembly of amphiphilic PEGylated hyperbranched poly(amidoamine)s can release doxorubicin at low pH or in the presence of high GSH concentration to kill cancer cells.